Nanoscale Res Lett (2010) 5:1257–1263
DOI 10.1007/s11671-010-9634-x

NANO EXPRESS

Fabrication of Porous Anodic Alumina with Ultrasmall Nanopores

Gu Qiao Ding · Rong Yang · Jian Ning Ding · Ning Yi Yuan · Yuan Yuan Zhu

Received: 14 January 2010 / Accepted: 5 May 2010 / Published online: 19 May 2010

Abstract Anodization of Al foil under low voltages of 1–10 V was conducted to obtain porous anodic aluminas (PAAs) with ultrasmall nanopores. Regular nanopore arrays with pore diameter 6–10 nm were realized in four different electrolytes under 0–30°C according to the AFM, FESEM, TEM images and current evolution curves. It is found that the pore diameter and interpore distance, as well as the barrier layer thickness, are not sensitive to the applied potentials and electrolytes, which is totally different from the rules of general PAA fabrication. The brand-new formation mechanism has been revealed by the AFM study on the samples anodized for very short durations of 2–60 s. It is discovered for the first time that the regular nanoparticles come into being under 1–10 V at the beginning of the anodization and then serve as a template layer dominating the formation of ultrasmall nanopores. Under higher potentials from 10 to 40 V, the surface nanoparticles will be less and less and nanopores transform into general PAAs.

Keywords Anodic alumina · Nanofabrication · Nanopore · Ultrasmall · Nanoparticle

G. Q. Ding (✉) · R. Yang · J. N. Ding (✉) · N. Y. Yuan · Y. Y. Zhu
Center for Low-Dimensional Materials, Micro-Nano Devices and System, Jiangsu Polytechnic University, 1 Ge Hu Road, Changzhou 213164, Jiangsu, China
e-mail: dingguqiao@gmail.com

J. N. Ding
e-mail: dingjn@jpu.edu.cn

G. Q. Ding · R. Yang · J. N. Ding · N. Y. Yuan · Y. Y. Zhu
Key Laboratory of New Energy Source, Changzhou 213164, China

Introduction

Self-ordered porous anodic alumina (PAA) has attracted considerable attention due to its utilization as a host or template to fabricate diverse nanostructures for different applications, such as electronic, magnetic and optoelectronic nanodevices [1–3]. The performance of related nanodevices relies on the dimensions of basic nanounits, such as nanodots, nanorods, nanowires and nanotubes. Generally, the performance will be significantly improved due to quantum effects when the nanounit's size is less than 10 nm [4, 5]. However, both the reported and commercialized PAAs have pore diameter ranging from 20 to 500 nm and corresponding interpore distance from 50 to 1000 nm [3, 6, 7], which is too large to fabricate nanounits with quantum effects. Consequently, it is necessary to fabricate PAAs with ultrasmall nanopores (pore diameter less than 10 nm). Furthermore, PAAs with ultrasmall nanopores have advantages over other methods to fabricate quantum dots and wires due to its low cost, high regularity, high sheet density and less requirements on depositing materials and methods [1, 3]. Conventional electron-beam lithography is workable, but expensive and impractical for large-scale fabrication [8]. Heteroepitaxial growth of quantum dots yields a sparse packing density and achieves only partial ordering with a broad distribution of dot sizes on some particular materials [9].

PAA Researchers have realized the value of ultrasmall nanopores and have tried to fabricate them. Some studies just obtained very thin layers (thickness 10–100 nm) of ultrasmall nanopores. Lira et al. claimed 5 nm pore size by applying electrical pulses at end of general PAA fabrication process [10]. According to the related SEM images, the claimed PAA layer is around 100 nm in thickness and the nanopores are not parallel to each other. Actually, it is a

new approach or a necessary step to open or remove the barrier layer. Kokonou et al. presented the fabrication of ultrasmall nanopores (5–10 nm) within ultrathin PAA layers (20–30 nm) in 6% (v/v) sulfuric acid at 20 V and in 6 wt% oxalic acid at 30 V for just few minutes of anodization [11]. Xu et al. proposed an expensive way of ion-milling the U-shaped bottom cap of the alumina nanochannel to obtain nanopore with a diameter as 10 nm [12], but the barrier layer was only 40 nm in thickness. Some researchers employed pretexturing techniques to obtain ultrasmall nanopores. Masuda et al. used a 2D Fe_2O_3 monodisperse nanoparticles as a template to leave a concave array on aluminum foil to obtain PAA with 13-nm pore intervals [13]. Asoh et al. fabricated highly ordered PAA films with 15 nm pore diameter by pretexturing Al with SiC mold and anodizing in 0.3 M sulfuric acid under a constant voltage of 25 V at 17°C [14]. Kim et al. employed much lower temperature of −15°C under 25 V in 0.3 M sulfuric acid to get PAAs with the pore diameter ~14 nm [15]. Ono et al. reported PAAs fabricated in different electrolytes at 2–40 V, and the pore diameter was claimed to be less than 10 nm by calculations according to the relationship between porosity and pore diameter [16]. In summary, pretexturing by metal, oxide or polymer [17] molds is workable to guide the growth the PAAs, but it is a complicated process, and it is also very difficult to get ultrasmall nanopores since it is hard to prepattern the surface with <10 nm textures. And so far, there is no direct evidence to confirm the formation of 1–10 nm ultrasmall nanopores by simple two-step anodization.

In this report, we present the simple two-step anodizing process to fabricate PAAs with ultrasmall nanopores. Atomic force microscopy (AFM), field emission scanning electron microscope (FESEM) and transmission electron microscopy (TEM) observations directly confirm the formation of ultrasmall nanopores (6–10 nm). Current evolution curves verify that these ultrasmall nanopores can be obtained in different electrolytes (oxalic acid and sulfuric acid with other additives) under wide potentials (1–10 V) and broad temperatures (0–30°C). The brand-new formation mechanism has been revealed according to the observation and analysis on the evolution of nanoparticles formed at the very beginning of the anodization.

Experimental Section

The samples were fabricated through a typical two-step electrochemical procedure with high-purity (99.999%) aluminum foil [2]. Prior to the anodization, the as-rolled foil was degreased in acetone and washed in deionized water. First anodization was carried out in different electrolytes for 30 min under the constant voltage of 1–10 V versus a graphite cathode. The specimens were then immersed in a mixture of 6.0 wt% H_3PO_4 and 1.8 wt% H_2CrO_4 at 60°C for 1 h to remove the oxide layers. The samples were then re-anodized under the same conditions for various durations. In order to obverse the ultrasmall nanopores from the bottom of PAA layer, we removed unanodized aluminum in a mixture of $CuSO_4$/HCl, and dissolved barrier layer in 5 wt% H_3PO_4 under 30°C for ~10 min to realize throughout free-standing membrane [17]. The surface and cross-sectional morphology of PAAs were characterized by AFM (Veeco, Nanoman VS system with TRESP probe), FESEM (Philips XL30FEG with a spatial resolution of 2 nm) and TEM (JEM-2010 with point resolution of 0.25 nm). The sample preparation and microscopy characterization skills have been detailedly presented in our previous work [18]. In addition, the current evolution curves were recorded by using a Keithley 2400 sourcemeter.

Results and Discussion

Figure 1 shows typical AFM bottom view of ultrasmall nanopores, which was obtained in 0.3 M oxalic acid under 15°C and 2 V for 30 min. Both the surface (Fig. 1a) and the 3D (Fig. 1b) morphology confirm the successful formation of ultrasmall nanopores. The pore diameter is about 4.4–10.0 nm with an average of 6.5 nm, and the average interpore distance is about 22.0 nm. As shown in Fig. 1a, these ultrasmall nanopores are not ordered circular holes, and the arrangement of the nanopores is not as good as general reported PAAs with highly ordered hexagonal cells [1, 3]. However, the growth rate of these nanopores should be the same since the height fluctuation is less than 10 nm in an area of 500 nm × 500 nm, as shown in Fig. 1c where the *X* and *Y* axes are combined [18]. Another typical PAA with ultrasmall nanopores was fabricated in the mixture of 20 wt% H_2SO_4, 1 wt% citric acid and 1 wt% $Al_2(SO_4)_3$ under 15°C and 10 V for 30 min. Both citric acid and $Al_2(SO_4)_3$ were added in order to avoid burning effect and stabilize the anodizing process [19]. After removing unanodized aluminum, the half-sphere barrier layer with an average diameter 24.2 nm is revealed, as shown in Fig. 1d. After dissolving the barrier layer, the ultrasmall nanopores can be characterized by AFM. Although the potential increased five times, the pore diameter (about 6.6–10.5 nm with an average 7.9 nm) and interpore distance of 26.2 nm do not significantly changed (Fig. 1e). It is very interesting that all the samples fabricated under 1–10 V have similar barrier layer thickness according to the same minimum erosion duration in H_3PO_4 for throughout membranes. Figure 1f verifies that only partial barrier layer is removed

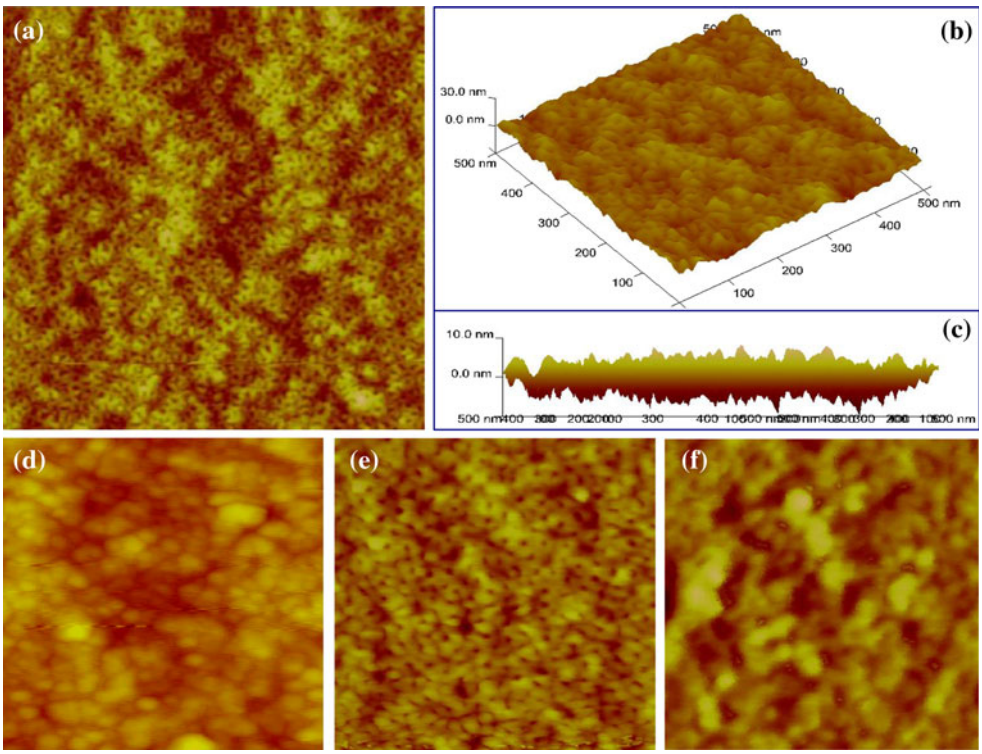

Fig. 1 AFM images of ultrasmall nanopores fabricated under 15°C and 2 V for 30 min in 0.3 M oxalic acid: **a** surface, **b** 3D image and **c** height profile by combining the *x*- and *y*- axis in (**b**). AFM images of ultrasmall nanopores prepared in the mixture of 20 wt% H_2SO_4, 1 wt% citric acid and 1 wt% $Al_2(SO_4)_3$ under 15°C and 10 V for 30 min: **d** as-prepared barrier layer, **e** immersed in 5 wt% H_3PO_4 for 10 min. **f** The barrier layer AFM image of PAA anodized in 0.3 M oxalic acid for 30 min under 1 V and immersed in 5 wt% H_3PO_4 for 6 min. The area of the AFM image in (**a**) is 1 μm × 1 μm, and the area of other images is 500 nm × 500 nm

after immersing the sample (anodized in 0.3 M oxalic acid at 1 V) in 5 wt% H_3PO_4 at 30°C for 6 min.

In order to further confirm the formation of ultrasmall nanopores, we used FESEM and TEM to characterize the PAA samples anodized at 10 V in 0.3 M oxalic acid. However, we could not see any nanopores on the surfaces of as-prepared samples under FESEM after a layer of gold was sputtered. So, the pore widening treatment was carried out at 30°C in 5 wt% phosphoric acid to facilitate the observation of nanopores' configuration. Figure 2a shows FESEM image of the sample immersed in phosphoric acid for 5 min. There are some ultrasmall nanopores and many ball-like nanoparticles well distributed on the surface with the average size of ~25 nm, which is obviously different from the flat porous surfaces of general reported PAAs. After pore widening in phosphoric acid for another 5 min, there are more ultrasmall nanopores observed, as shown in Fig. 2b. The cross-sectional view FESEM image of Fig. 2c verifies that the nanopores are parallel to each other. TEM image of Fig. 2d exhibits the morphology of the free-standing ultrathin PAA after both the aluminum base and the half-spherical barrier layer were removed, and the pore diameter was widened in phosphoric acid for 10 min.

The above AFM, FESEM and TEM images are typical ones to verify the formation of ultrasmall nanopores. In fact, we have fabricated many PAAs with ultrasmall nanopores in four different electrolytes (0.3 M $H_2C_2O_4$/1 M H_2SO_4/20 wt% H_2SO_4 + 1 wt $Al_2(SO_4)_3$/20 wt% H_2SO_4 + 1 wt% citric acid + 1 wt% $Al_2(SO_4)_3$) at various temperature from 0 to 30°C and different potentials from 1 to 10 V. The sulfuric acid itself with different concentrations was generally used to get PAAs with small nanopores [20, 21]. Al ions and citric acid can be the stabilizer to avoid burning effect. Oxalic acid is the mostly reported electrolyte for highly ordered PAA fabrication, especially for 40 V mild anodization [2, 17]. Current evolution curves were tracked to confirm whether steady-state anodization can be obtained and how the current density varied during the anodization. Figure 3 shows the current–time curves under anodizing potentials from 1 to 10 V and broad temperature of 0–30°C in 0.3 M oxalic acid. The current density decreases rapidly at the beginning and then maintains at a steady-state current, while the typical current evolution firstly experiences a rapid drop to lowest point and then increases slowly to a constant value [17]. According to these curves, the stable anodizing process can be achieved under various conditions and that the growth rate of the PAA can be increased by raising the electrolyte temperature and applied potential.

It is well known that there are some general rules for the PAA fabrications, but the fabrication of ultrasmall nanopores breaks these rules including:

1. For general PAAs, both the pore diameter (1 nm/V) and interpore distance (2.0–2.5 nm/V) are proportional to the applied potential. However, for ultrasmall

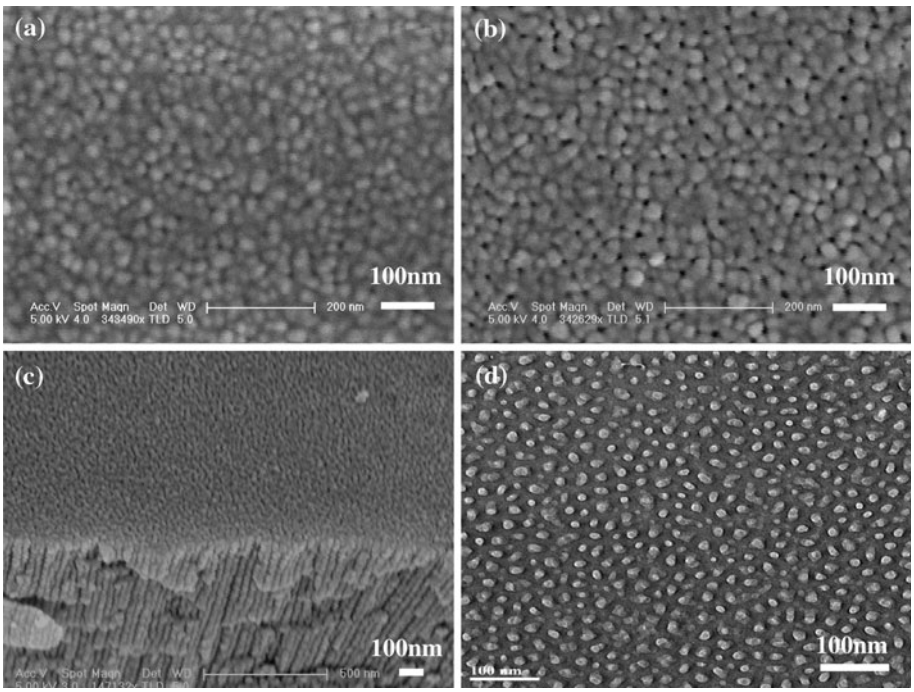

Fig. 2 FESEM *top view* images of ultrasmall nanopores prepared in 0.3 M oxalic acid under 10 V for 30 min and pore-widened in 5 wt% H_3PO_4 for 5 min (**a**) and 10 min (**b**), respectively, **c** oblique view of (**b**) and **d** TEM image of free-standing ultrasmall nanopores prepared in 0.3 M oxalic acid under 10 V for 5 min and pore-widened in 5 wt% H_3PO_4 for 10 min after removing the un-anodized aluminum and barrier layer

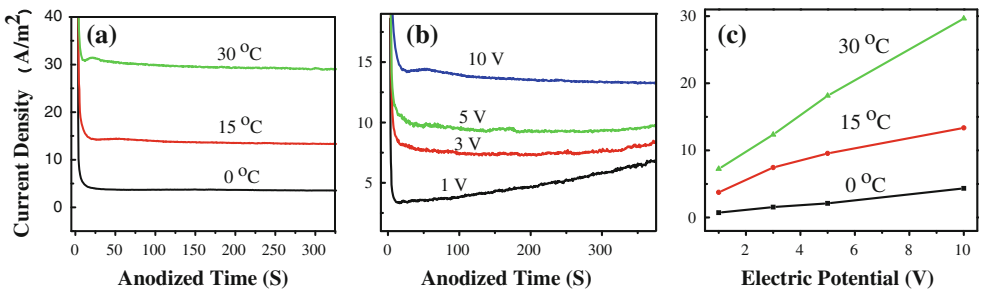

Fig. 3 Current evolution curves during the second-time anodization in 0.3 M oxalic acid: **a** under 10 V with different temperature, **b** 15°C with different potentials and **c** the current density-potential relationship under different temperature

nanopores, the average pore diameter and interpore distance remain 6–10 and 20–30 nm, respectively, when the potentials varies from 1 to 10 V.

2. The thickness of barrier layer is linear with the applied potential for general PAAs, while it is around 10 nm no matter how the potentials changes from 1–10 V for ultrasmall nanopores.
3. It is well known that 0.3 M $H_2C_2O_4$ is used under 40 V or higher and that H_2SO_4 is used under 25 V or higher. We can obtain ultrasmall nanopores in both oxalic and sulfuric acids with or without other additives. The anodization process is not sensitive to the electrolytes, and the electrolyte composition is not a key factor for the formation of ultrasmall nanopores although it is very important for the growth rate.

In addition to rule-breaking behaviors, the current evolution curves during fabricating ultrasmall nanopore are also different from general ones. So, the formation mechanism under 1–10 V should be different. In order to reveal the real formation process, we prepared the samples in 0.3 M oxalic acid at 1–10 V with short second-anodizing durations (2, 5, 10, 20 and 60 s) and conducted AFM tests to figure out the nucleation and growth process of ultrasmall nanopores. Figure 4a is the AFM image of the sample anodized at 2 V for 5 s. It is clear that some nanoparticles come into being on the surface, and these nanoparticles grow up and cover the whole surface after 20 s (Fig. 4b). As the potential increases to 10 V, the nanoparticles have uniform shape and cover the whole surface after just 10 s (Fig. 4c). Under the potentials of 1–10 V, these nanoparticles remain its size and shape even after long-time anodizations (30 min, 2 and 10 h), which was conformed by AFM tests. It is discovered for the first time that the regular nanoparticles come into being under 1–10 V at the beginning of the anodization.

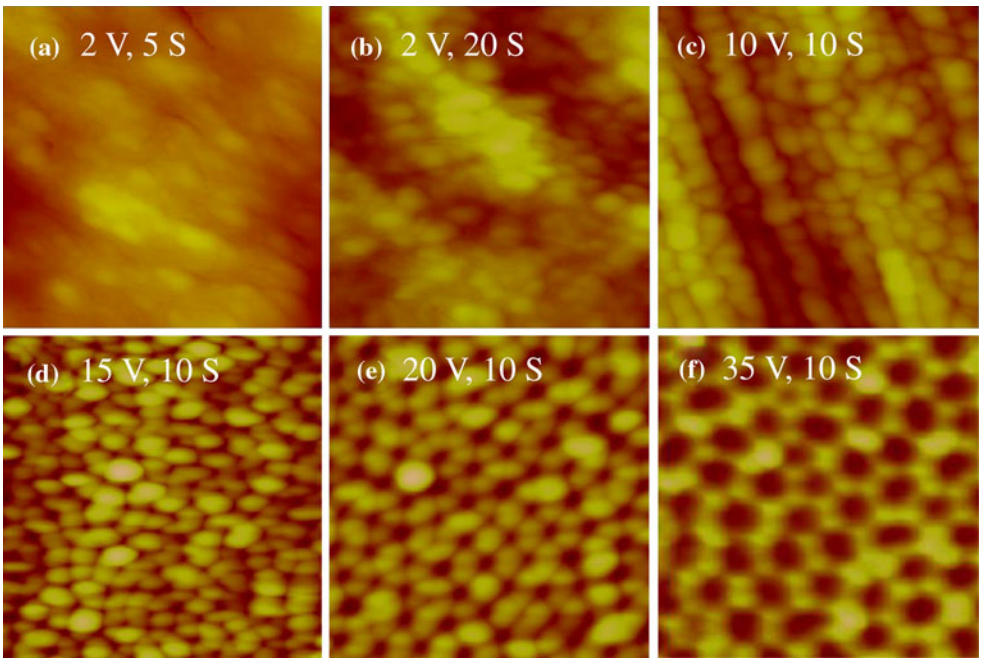

Fig. 4 AFM images with an area of 250 nm × 250 nm of PAAs fabricated under **a** 2 V for 5 s, **b** 2 V for 20 s and **c** 10 V for 10 s in 0.3 M oxalic acid, AFM images with an area of 500 nm × 500 nm under **d** 15 V, **e** 20 V and **f** 35 V for 10 s in 0.3 M oxalic acid, respectively

Since both the formation rate and size of these nanoparticles should depend on the applied potentials, we further study the PAA samples anodized under 10–40 V in 0.3 M oxalic acid. Figure 4d is the AFM image of PAA fabricated at 15 V, and the nanopores come into being although there are still lots of nanoparticles about 27.1 nm in diameter on the surface. Under higher potentials of 20 and 35 V, the nanopores grow up and transform into ordered hexagonal cell structure with less nanoparticles, as shown in Fig. 4e and f. In order to make a comparison with the general PAA, we fabricated PAA in 0.3 M oxalic acid under 40 V for 10 h and tested the surface. There are also some nanoparticles on its surface although its sheet density is very low (5 per μm^2), as shown in Fig. 5a. Generally, under 1–10 V, the nanoparticles (20–30 nm) can cover the sample surface as a mask or template, and ultrasmall nanopores (<10 nm) can be obtained. As the potential increases from 10 to 40 V, the regularity of nanopores is gradually improved while the nanoparticles become less and less. The sheet density of the nanoparticles on the PAA surface is estimated to be $1.4 - 2.4 \times 10^{11}$ per cm^2 when the anodizing potential varies from 1 to 10 V, and it decreases to $\sim 5 \times 10^8$ per cm^2 when the potential is 30–40 V. The relationship between pore diameter/nanoparticle size and anodizing potential is given in Fig. 5b based on the AFM results.

According to above results, the most important difference between general and the obtained ultrasmall nanoporous PAAs is the formation of nanoparticles on the surface at the very beginning of the anodization. When these nanoparticles grow up to about 20–30 nm and cover the whole surface, they become stable in shape and size and remain until the end of the anodization. It is these nanoparticles that dominate the forming process of ultrasmall nanopores since the ultrasmall nanopores can only nuclear and grow up at the gaps between these nanoparticles. The ultrasmall nanopores have similar pore diameter under 1–10 V because both the shape and size of these nanoparticles do not vary much after their formation. This nanoparticle layer acts as a template for the formation of ultrasmall nanopores, which is similar to the nanoscale prepatterns on the aluminum surface before anodization by Fe_2O_3 [13], SiC [14], PMMA [22] and metal molds [23].

To further confirm that the nanoparticle's functionality is a template during the formation of ultrasmall nanopores, we first conducted the second anodization at 5 V for 20 s to form a layer of uniform nanoparticles, then anodized the sample at 20 V for 1 h (Fig. 5c), or increased the potential to 40 V with a speed of 15 V per minute and maintained at 40 V for 1 h (Fig. 5d). Obviously, these samples have totally different surfaces with their counterparts without pretexturing nanoparticle layers as shown in Figs. 4e and 5a. Although the potentials increase to 20 and 40 V and the corresponding current densities increase to 20 and 50 A/m^2, these nanoparticles cannot be removed after 1 h anodization. Similar template effect was utilized by

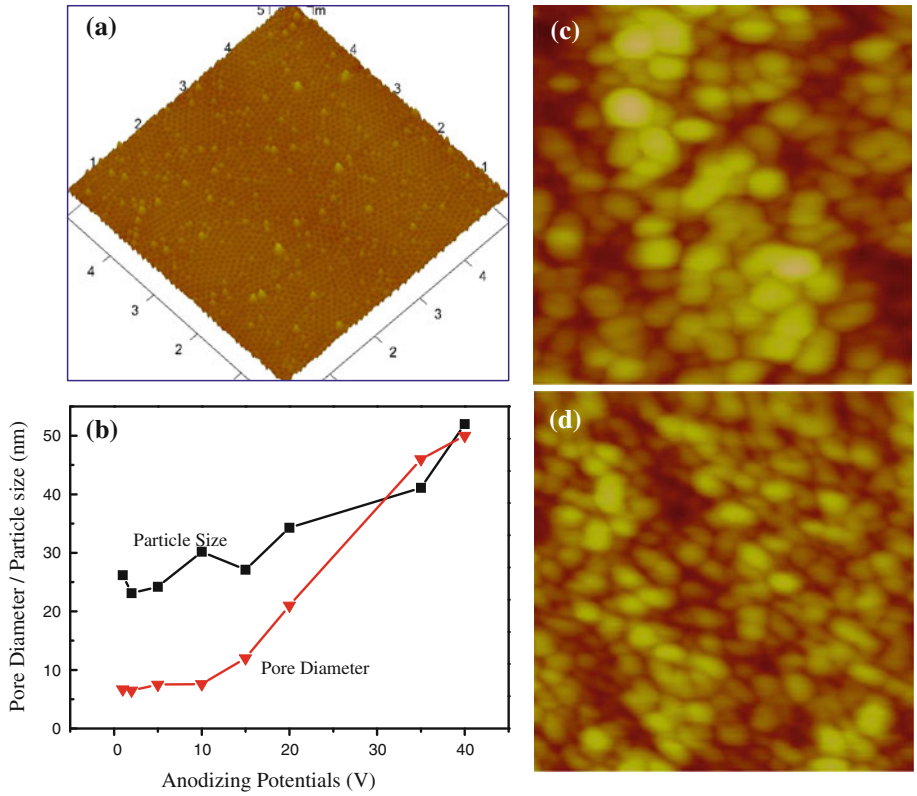

Fig. 5 **a** 5 μm × 5 μm AFM images PAA fabricated in 0.3 M oxalic acid under 40 V for 10 h, **b** the relationship between nanoparticle size/pore diameter and anodizing potentials, 500 nm × 500 nm AFM images of PAAs re-anodized under **c** 20 V and **d** 40 V for 1 h after 20-s anodization at 5 V

pretexturing the aluminum surface to obtain different pore arrangement or different pore shapes since prepatterns will restrict the distribution of electric field [22, 23].

For fabricating PAA with ultrasmall nanopores, the growth rate is also very critical. According to our study [17], the growth rate in oxalic acid can be improved by raising the electrolyte temperature and applied potential. For example, at 0°C and 3 V, the growth rate is about 0.5 μm/h, and it can be improved to be 3 μm/h under 30°C and 10 V. But in the case of sulfuric-acid-based electrolyte, the theoretical estimation is very difficult since as the electrolyte temperature and applied potential increase, the chemical erosion on the PAA membrane is also significantly enhanced. According to FESEM measurements, typical growth rate is estimated to be 0.2–1 μm/h under 0–30°C in 1–20 wt% sulfuric acid. Generally, the highest growth rate of 3 μm/h in oxalic acid is still too low for manufacture when compared to the reported hard anodization [24] and high field anodization [25–27] under higher potentials. A fast fabricating method of PAAs with ultrasmall nanopores in oxalic acid has been developed by improving the anodizing potential to 60–70 V after short-time anodization under 1–10 V, and the growth rate can be enhanced to be as high as 30 μm/h while pore diameter remains unchanged. The detailed experimental information and results will be given in another report.

Conclusions

In summary, PAAs with ultrasmall nanopores of 6–10 nm were fabricated in various electrolytes under 1–10 V and 0–30°C according to the AFM, FESEM, TEM images and current evolution curves. The pore diameter (6–10 nm), interpore distance (20–30 nm) and the barrier layer thickness (~10 nm) do not vary significantly when the applied potential varies in the range of 1–10 V. The regular nanoparticles (20–30 nm) form at the very beginning of the anodization, cover the whole surface, remain their shape and size and act as a template layer dominating the formation of ultrasmall nanopores during the rest of the anodization. The nanoparticles will be less and less, and the nanopores transform into general PAAs when the potential is increased from 10 to 40 V.

Acknowledgments This work was supported by New Century Excellent Talents (NCET-04-0515), Qing Lan Project (2008-04), Key Programs for Science and Technology Development of Jiangsu (BE20080030), Changzhou Science and Technology Platform (CM2008301) and Key Laboratory of Material Tribology of Jiangsu (KJSMCX0902).

References

1. H. Chik, J.M. Xu, Mater. Sci. Eng. R **43**, 103 (2004)
2. H. Masuda, M. Satoh, Jpn. J. Appl. Phys. **35**, L126 (1996)
3. Y. Lei, W. Cai, G. Wilde, Prog. Mater. Sci. **52**, 465 (2007)
4. L.J. Wang, A. Rastelli, S. Kiravittaya, M. Benyoucef, O.G. Schmidt, Adv. Mater. **21**, 2601 (2009)
5. N. Tomczak, D. Jańczewski, M. Han, G.J. Vancso, Prog. Ploym. Sci. **34**, 393 (2009)
6. S.Z. Chu, K. Wada, S. Inoue, M. Isogai, Y. Katsuta, A. Yasumori, J. Electrochem. Soc. **153**, B384 (2006)
7. Y. Li, Z.Y. Ling, S.S. Chen, X. Hu, X.H. He, Chem. Commun. **46**, 309 (2010)
8. J.Y. Liang, H. Chik, J. Xu, IEEE J. Sel. Quant. **8**, 998 (2002)
9. J.Y. Liang, H. Chik, A. Yin, J. Xu, J. Appl. Phys. **91**, 2544 (2002)
10. H.L. Lira, R. Paterson, J. Membrane Sci. **206**, 375 (2002)
11. M. Kokonou, K.P. Giannakopoulos, A.G. Nassiopoulou, Thin Solid Films **515**, 3602 (2007)
12. T. Xu, G. Zangari, R.M. Metzger, Nano. Lett. **2**, 37 (2002)
13. H. Masuda, Y. Matsui, K. Nishio, Small **2**, 522 (2006)
14. H. Asoh, K. Nishio, M. Nakao, A. Yokoo, T. Tamamura, H. Masuda, J. Vac. Sci. Technol. B **19**, 569 (2001)
15. T.Y. Kim, S.H. Jeong, J. Chem. Eng. **25**, 609 (2008)
16. S. Ono, N. Masuko, Surf. Coat. Tech. **169–170**, 139 (2003)
17. G.Q. Ding, M.J. Zheng, W.L. Xu, W.Z. Shen, Nanotechnology **16**, 1285 (2005)
18. Y.Y. Zhu, G.Q. Ding, J.N. Ding, N.Y. Yuan, Nanoscale Res. Lett. **5**, 725 (2010)
19. S. Ono, M. Saito, H. Asoh, Electrochem. Solid-State Lett. **7**, B21 (2004)
20. H. Masuda, F. Hasegwa, S. One, J. Electrochem. Soc. **144**, L127 (1997)
21. G.D. Sulka, S. Stroobants, V. Moshchalkov, G. Borghs, J.P. Celis, J. Electrochem. Soc. **149**, D97 (2002)
22. J.T. Smith, Q.L. Hang, A.D. Franklin, D.B. Janes, T.D. Sands, Appl. Phys. Lett. **93**, 043108 (2008)
23. K. Yasui, K. Nishio, H. Nunokawa, H. Masuda, J. Vac. Sci. Technol. B **23**, L9 (2005)
24. W. Lee, R. Ji, U. Gösele, K. Nielsch, Nat. Mater. **5**, 741 (2006)
25. S.Z. Chu, K. Wada, S. Inoue, M. Isogai, A. Yasumori, Adv. Mater. **17**, 2115 (2005)
26. Y. Li, Z.Y. Ling, S.S. Chen, J.C. Wang, Nanotechnology **19**, 225604 (2008)
27. Y.B. Li, M.J. Zheng, L. Ma, W.Z. Shen, Nanotechnology **17**, 5101 (2006)